Thermodynamic Analysis of Refrigerant-DMF Solutions in Solar-Driven Absorption Refrigeration System

Lijuan He, Yazhu Zhang, Wenfei Wu[1],

Institute of Environment and Energy, Inner Mongolia University of Science and Technology, Baotou, China

Corresponding author: *wwf@imust.cn*

Abstract: Thermodynamic performances of a solar driving single-stage and intermittent absorption refrigerator using R22+DMF, R134a+DMF, R32+DMF as working fluids were analyzed respectively. The circulation ratio f was considered as an additional optimization parameter. The results show that R134a+DMF mixture may be considered as a good candidate for application to solar refrigeration systems due to its relative low pressure and higher coefficient of performance. It will present interesting properties at moderate condensing and absorbing temperatures (298K-308K) when the evaporating temperature in the range from 278K to 288K which are highly useful for food preservation and for air conditioning in rural areas.

Keywords: Solar refrigeration; Modified intermitted system; Parametric study

1 Introduction

Solar energy can be transformed either to electricity or to heat to power a refrigeration cycle. However, the technology for the conversion from solar energy to electrical energy to cooling a load has not been accomplished economically so far. An absorption refrigeration system can utilize heat directly as the driving energy for cooling purposes. The solar-powered absorption systems have been studied by many researchers [1-5].

In absorption refrigeration cycles, it is important to select appropriate working fluids. H_2O-LiBr and NH_3-H_2O are well known two major working pairs used in the solar absorption refrigeration systems. The NH_3-H_2O system is more complicated than the H_2O-LiBr system since a rectifying component is needed to assure no water vapor enters the evaporator, and requires a generating temperature in the ranges of 125℃-170℃ for air-cooling in the absorber and condenser or 95℃-120℃ for water-cooling. The coefficient of performance (COP) of the system is from 0.6 to 0.7 for single-effect and single-stage systems. The H_2O-LiBr system operates at a lower generating temperature in the range of 70℃-95℃ when cooling water is used as a coolant. The higher COP of 0.6-0.8 may be obtained for a single effect system[6]. However, the evaporator of H_2O-LiBr system cannot be operated at a temperature much below 5℃ since the refrigerant is water. Generally speaking, NH_3-H_2O systems are often used for industrial applications while H_2O-LiBr systems are more suitable for air-conditioning purposes.

Besides, some new working pairs have also been investigated. Worsoe-Schmidt and Erhard et al. developed a solar-powered solid-adsorption refrigeration system with NH_3-$CaCl_2$ and NH_3-$SrCl_2$ as working pairs with an overall COP of 0.10 and 0.045-0.082, respectively[7,8]. Romero employed an aqueous ternary hydroxide working fluid in the proportion of 40:36:24 (NaOH:KOH:CsOH) in a solar absorption cooling system with a higher COP than that with the H_2O-LiBr mixture[9].

Rivera carried out a theoretical study of an intermittent absorption refrigeration system[10], which was driven by a compound parabolic concentrator operated with $LiNO_3$ mixture in order to avoid a rectifier. The results show that the COPs of the system were between 0.15 and 0.4 depending on the generating and condensing temperatures.

Medrano reported a double-lift absorption cycle of using organic fluid mixtures，trifluoroethanol(TFE）-tetraethylenglycol dimethylether(TEGDME or E181) and methanol-E181 as working pairs[11]. The simulation results show that the COP with TFE-E181 is 15% higher than that with NH_3-H_2O.

In present study, the simulation of an absorption refrigeration cycle under different operating conditions was

* Project supported by the Innovation Foundation of the Inner Mongolia University of Science and Technology (No. 2009NC003)

carried out for binary mixtures of R22, R32 and R134a with Dimethylformamide (DMF) respectively. The above working pairs are of great advantages to reduce system pressure and to use solar energy as energy supply in the system, in addition to chemically stable, non-corrosion, completely miscible in a wide temperature range[12]. The thermodynamic properties of each pure refrigerant may be obtained from the software Refprop.7.1. The thermodynamic properties and VLE data of binary mixtures have been reported by L.J. He and X.L Cui respectively[13,14].

2 Simulation Expressions of Solar-driven Absorption Refrigeration

The conventional heat driven single-stage absorption refrigeration system consists of a generator, a condenser, an evaporator, an absorber and a solution heat exchanger as shown schematically in Fig.1. The numbers in Fig.1 denote the state points which are used in the analysis.

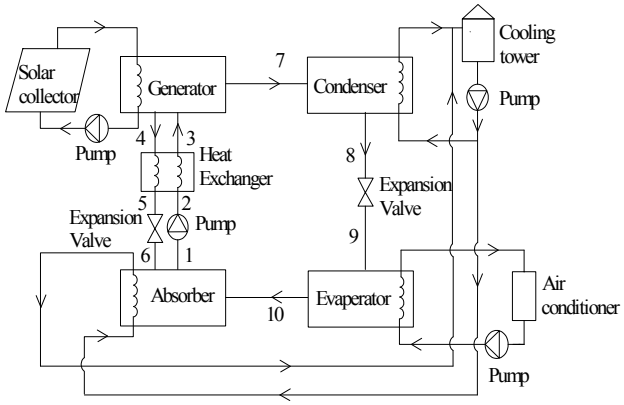

Fig.1 Scheme of the solar-driven absorption refrigeration system

In the hot water circuit, the solar energy is absorbed by the collector and accumulated in the storage tank. Then the low grade thermal energy supplies to the generator so as to remove the refrigerant vapor. Once the solution in the generator reaches its generating temperature, pure refrigerant vapor goes into the condenser and gets to be condensed. The refrigerant liquid from the condenser expands through the expansion valve and enters the evaporator, in which the refrigerant takes the cooling load and vaporizes again. The vapor then goes into the absorber.

In the absorber, the weak solution absorbs the refrigerant vapor, and the heat of mixing and condensation is removed by cooling water from the cooling tower. The strong solution is pumped from the absorber by a mechanical pump and preheated by the weak solution in the heat exchanger and then goes to the generator.

In order to make the chiller more suitable use of solar energy, the cooling water circulations in the condenser and absorber are arranged in parallel. A hot water storage tank is used to store heat collected from the collector and to make the system running under a comparatively stable condition. This cycling process goes on until the sunshine is not available.

The performance simulation is performed based on two main circulations of the system, namely, the solar collector circulation and the chiller circulation including cooling water circuit, chilled water circuit and solution circuit.

2.1 Collector circulation

The solar collector characterized by its efficiency η_{se} and surface area A_{se} is used to increase the hot water supply temperature from T_r to T_h. The collector efficiency is assumed as[15]:

$$\eta_{se} = 0.8 - 5.7\frac{0.5(T_r + T_h) - T_{am}}{I} \quad (1)$$

$$T_r = T_h - \Delta T_{ss} \quad (2)$$

Substituting Eq (2) into Eq. (1), yields:

$$\eta_{se} = 0.8 - 5.7\frac{T_h - 0.5\Delta T_{ss} - T_{am}}{I} \quad (3)$$

where ΔT_{ss} is generating temperature glide and T_h is 5K higher than T_g.

The solar collector circulation consists of a flat plate collector array and a hot water tank. The collectors are tilted at the latitude 30°23’ in Hangzhou, where the maximum ambient temperature occurs in July and the maximum solar radiation on a horizontal surface is 830W/m^2 year round.

978-1-935068-37-2 © 2010 SciRes.

2.2 Chiller Circulation

The chiller circulation consists of a 1.0 kW nominal cooling capacity single-stage absorption chiller and a cooling tower. A mathematical model is developed to simulate the performance of the system shown in Fig.1. Some assumptions are made for the development of the model and described as follows:

The condenser and the absorber operate at the same temperature;

Refrigerant liquid at point 8, refrigerant vapor at point 10, refrigerant-DMF at points 1 and 4 are under saturated conditions corresponding to the respective temperatures and pressures;

No DMF exists in the refrigerant loop;

Heat losses to ambient, pressure drops and work required to pump the strong solution are negligible.

The performance simulation model is established from heat and mass balances for each component of the cycle. The enthalpies at the inlet and outlet of each component are calculated based on the thermodynamic properties of refrigerant and refrigerant-absorbent mixtures. The properties of pure refrigerants are obtained from the software Refprop7.1. Thermodynamic properties of pure liquid DMF are taken from X.L Cui[16]. Enthalpy data h_{DMF} are correlated as a function of absolute temperature as follows:

$$h_{DMF} = a_1 + a_2 T + a_3 T^2 \quad (4)$$

where , T is absolute temperature, a_1=-297.61, a_2=0.89544, a_3=0.0020551.

Thermodynamic data of mixtures are rarely reported. The expressions of enthalpy of mixtures are taken from Tyagi [17] and expressed as follows:

$$h_{Ref.+DMF} = x h_{Ref.} + (1-x) h_{DMF} + h_{mix} \quad (5)$$

$$h_{mix} = \frac{R(1-X)}{MX+73.09(1-X)}\{(f_0 + 2\frac{g_0}{T} - c_2 - c_3 T^2 + c_4 T)\frac{X}{1-X} + (f_1 + \frac{2g_1}{T})[\frac{X}{1-X} + ln(1-X)] + (f_2 + \frac{2g_2}{T})[\frac{1}{1-X} - (1-X) + 2ln(1-X)]\} \quad (6)$$

where $h_{Ref.+DMF}$ is enthalpy of mixture, h_{mix} is integral mixing heat of the two liquids, h_{DMF} is enthalpy of pure liquid DMF, $h_{Ref.}$ is enthalpy of liquid refrigerant, T is absolute temperature, R is universal gas constant, M is molecular weight of pure refrigerant. The rest numerical constants are listed in Table 1.

The equilibrium vapor pressure of refrigerant in DMF solution is expressed as:

$$p_{eq} = exp\left[\sum_{n=0}^{2} e_n X^n + \frac{1}{T}\sum_{n=0}^{2} f_n X^n + \frac{1}{T^2}\sum_{n=0}^{2} g_n X^n\right] \quad (7)$$

where p_{eq} is pressure, X is liquid mole fraction of refrigerant in DMF and constants are also listed in Table 1.

Based on Eqs.(6) and (7), thermodynamic properties of refrigerant, absorbent and refrigerant-absorbent mixture may be derived. If two among these parameters (p,T, x, h) are known, the others may be calculated.

Table 1 Numerical constant for Equations (6) and (7)

	c_2	c_3	c_4	e_0	e_1	e_2	f_0	f_1	f_2	g_0	g_1	g_2
R22	-3835.1	0.012	-8.6	19.7	-62.6	158.7	-3504.4	32838.1	-12259.7	656962.9	-1150373.0	-7367276.7
R32	-4098.1	0.019	-11.5	18.3	-50.3	119.0	-3790.2	31032.9	-14570.1	678505.6	-1451003.7	-7629785.6
R134a	-4818.8	0.018	-12.6	24.5	-73.0	141.3	-3459.8	24329.4	-18891.9	610136.4	-1112593.9	-7577562.2

The principal equations used in the calculation of mass and energy balances for each component of the refrigeration system are shown in Table 2.

2.3 Performance characteristics of a single-stage absorption refrigerating system

Coefficient of performance and circulation ratio are two key factors describing the efficiency of a solar absorption system. The overall COP of a solar absorption refrigerator is equal to the product of solar collector efficiency (η_{se}) and coefficient of performance COP_{th} defined as follows [18]:

$$COP = \eta_{se} COP_{th} \quad (9)$$

Neglecting pumping work, COP_{th} of the system is calculated as follows:

$$COP_{th} = \frac{\text{cooling power}}{\text{energy received by system}} = \frac{q_e}{q_g} \quad (10)$$

The circulation ratio which determines physical di-

mensions and pumping requirement is defined as follows:

$$f = \frac{m_1}{m_7} \tag{11}$$

Table 2 Mass and energy balances for various components of absorption cycle

Component	Mass balance	Energy balance	Assumption
Generator	$m_3=m_4+m_7$ $m_3x_3=m_7x_7+m_4x_4$	$q_g = h_7 + (f-1)h_4 - fh_3$	$T_g=T_4=T_7$ $p_g=p_c$,, $x_4=x_w$
Condenser	$m_7=m_8$ $m_7x_7=m_8x_8$	$q_c=h_8-h_7$	$T_8=T_c$ $x_c=x_7=x_8$
Evaporator	$m_9=m_{10}$ $m_9x_9=m_{10}x_{10}$	$q_e = h_{10} - h_9$	$h_8=h_9$ $p_e=p_{10}$, $x_9=x_{10}$
Absorber	$m_1=m_6+m_{10}$ $M_1x_1=m_6x_6+m_{10}x_{10}$	$q_a=h_{10}+(f-1)h_6-fh_1$	$h_1=h_2$, $h_5=h_6$ $x_1=x_2=x_s$, $x_5=x_6=x_w$
Solution heat exchanger	$m_2=m_3$ $m_4=m_5$	$q_{ex}=(f-1)(h_4-h_4)=f(h_3-h_2)$ $m_2h_2+m_4h_4=m_3h_3+m_5h_5$	$x_2=x_3$, $x_4=x_5$
Expansion valve	$m_5=m_6$ $m_8=m_9$	$h_5=h_6$ $h_8=h_9$	$\triangle_{WEV}=0$
Pump solution	$m_1=m_2$	$h_8=h_9$	$\triangle_{Wp}=0$

3 COMPUTED RESULTS AND DISCUSSION

Once condensing, absorbing and evaporating temperatures are fixed, a range of generating temperature at which the cycle can be operated is determined. The functional dependences of *COP* and circulation ratio *f* upon generating temperature T_g, condensing temperature T_c and evaporating temperature T_e may be computed and the results are presented in Fig.2 and Fig.3.

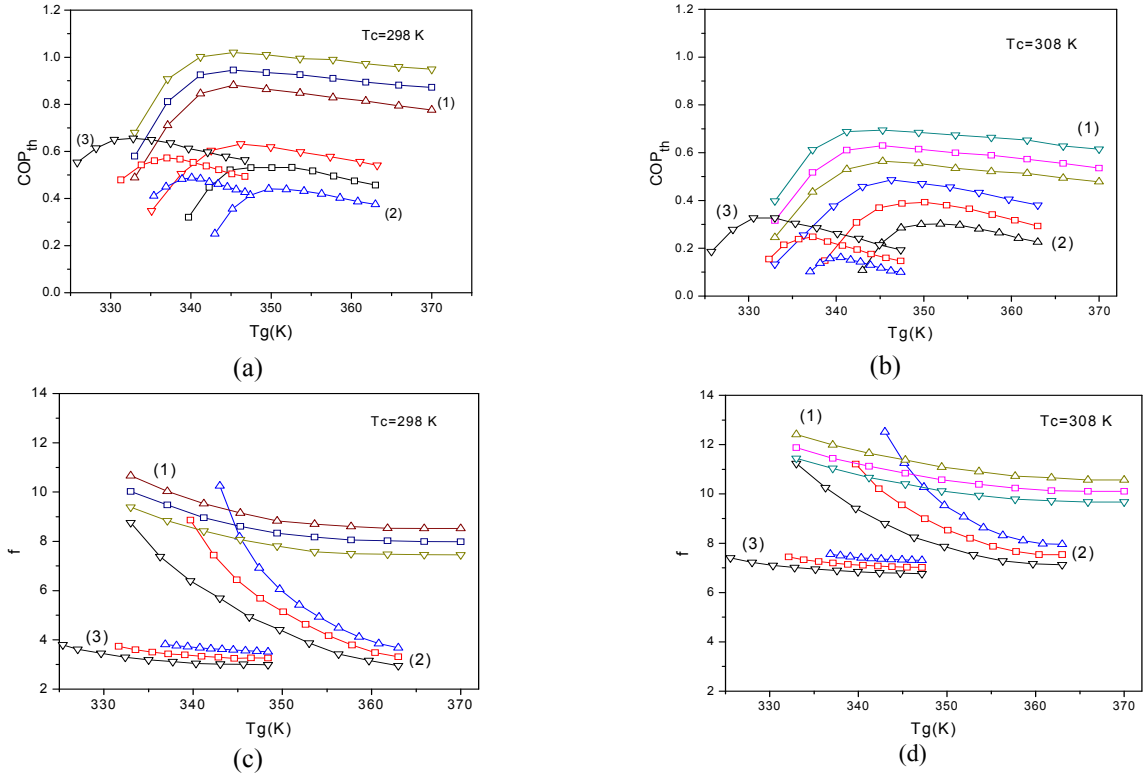

Fig. 2 Effect of operating temperature on system characteristics at different T_c and Te
(1)R134a+DMF (2)R22+DMF (3)R32+DMF △, T_e =278K; □, T_e =283K; ▽, T_e =288K

It is instructive to compare the overall performance characteristics of the absorption refrigeration unit operating with R22+DMF, R134a+DMF, R32+DMF, respectively. Figs 2(a)-(b) show that *COPs* increase with in-

978-1-935068-37-2 © 2010 SciRes.

crease of evaporating temperature T_e and decrease of condensing temperature T_c, and an optimum generating temperature T_g to the maximum *COP* point of the system can be found . In reverse, the circulation ratio *f* increases with decrease of T_e and increase of T_c as shown in Figs.2 (c)-(d).

Thus, the curves in Fig.2 permit one to evaluate and select the most feasible conditions for operation of the refrigeration cycle based on refrigerant-absorbent pairs. Evidently, the conditions under which the *COP* and *f* curves must show a minimum variation with generating temperature T_g must be stable for operation. As shown in Table 3, at the same condensing and evaporating temperatures, the generating temperatures of system R32+DMF are the lowest. Obviously, the system R32+DMF is more stable than R134a+DMF and R22+DMF.

Table 3 Generating temperature Tg of absorption refrigeration cycle under different operating conditions,(K)

Condensing temperature (K)	T_c	R134a+DMF Evaporating temperature T_e(K)			R22+DMF Evaporating temperature T_e(K)			R32+DMF Evaporating temperature T_e(K)		
		298	303	308	298	303	308	298	303	308
278		345	346	349	349	348	351	340	341	342
283		343	344	346	344	345	348	336	337	338
288		340	341	343	341	342	345	330	331	332

As shown in Fig.2(a)-(b), the *COP* of system R32+DMF are the highest only in the range of generating temperature T_g＝326K-348K. However, the circulation ratio *f* of the system R32+DMF is substantially low at condensing (T_c=298-303K) and evaporating temperatures (T_e=278-288K) as shown in Figs.2 (c)-(d).

The COP of the system R22+DMF shown in the Fig.2 (a)-(b) is the lowest within operating temperature range of 333K-363K and the circulation ratio of the system R22+DMF shown in Fig.2 (c)-(d) increases sharply. For a stable operation of the system, it is advisable to operate in the flat region of the curves in Fig2 (c)-(d).

Inspection for all generating temperatures shows that in all cases the *COP* of the system R134a+DMF is the highest in generating temperature range (T_g=333K-370K) and its corresponding circulation ratio *f* increases comparatively evenly.

In fact, for given values of T_c and T_e, a limiting lower value of T_g exists at which the system can not work and the *COP* plunges to zero duo to the absence of refrigerant vapor. Such limiting values of operating temperatures for the complete range of parameters are shown in Fig.3. For any given T_c and T_e, the corresponding limiting temperature value can be estimated from Fig.3. It shows that the generating temperature of system R134a+DMF is the widest and that of system R32+DMF is the narrowest.

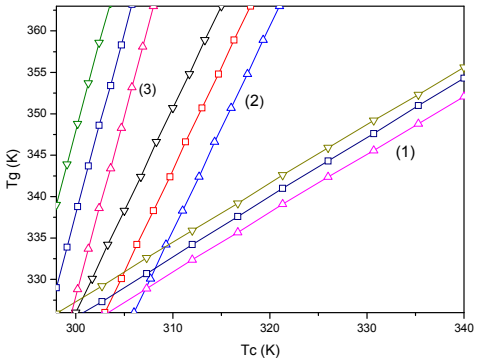

Fig. 3 Operating temperature range (1) R134a+DMF (2) R22+DMF (3) R32+DMF △, Te =278K; □, Te =283K; ▽, Te =288K

The last characteristic studied in the paper is the annual refrigeration capacity of the whole system shown in Fig.4. It indicates that the monthly variation of the refrigeration capacity for the same evaporation temperature (278K) and the different optimum generating temperatures while the corresponding COP*s* of the whole systems are the maximum. The refrigeration capacity of the system R134a+DMF reaches a maximum monthly value of 312KJ in July.

Accordingly, it may be concluded that the system R134a+DMF gives the best performance characteristic. This study supports the supremacy of R134a+DMF as the absorbent-refrigerant pair.

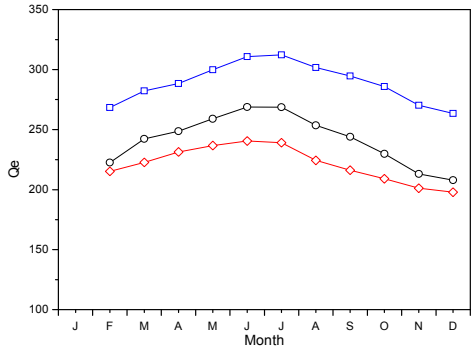

Fig. 4 Monthly variation of refrigeration capacity □,R134a+DMF ◇,R22+DMF ○,R32+DMF

4 Conclusions

The thermodynamic analysis of the absorption refrig-era-tion cycle helps us to estimate the performance of the refrigeration system. The comparative study of cycle performances for various mixtures shows that the overall coefficient of performance of R134a+DMF mixture is the highest and its circulation ratio f decreases with an in-crease in the generating and evaporating temperatures and with a decrease of the absorbing and condensing temperatures. The mixture R134a+DMF presents in-ter-esting thermodynamic properties for its application in absorption systems at moderate condensing and ab-sorb-ing temperatures (298K-308K).These performances are highly useful for medical and food product preserva-tion and for air conditioning. Therefore, the R134a+DMF mixture can be considered as a good candidate working pair for application to solar refrigeration systems.

References

[1] Kapur J.C., A report on the utilization of solar energy for refrig-eration and air conditioning application. *Solar Energy,* 1960,4, 39-47.

[2] Uppal A.H., Norton B. and Probert S.D. , A low-cost solar-energy stimulated absorption refrigerator for vaccine storage. *Appl. En-ergy,* 1986,25, 167-174

[3] Yeung M.R., Yuen P.K., Dumm A. and Cornish L.S., Perform-ance of a solar-powered air conditioning system in Hong Kong. *Solar Energy, 1992,* 48, 309-319.

[4] Syeda A., Izquierdod M., Rodriguez P., Maidment G., Missenden J. and Lecuona A., A novel experimental investigation of a solar cooling system in Madrid. *Int. J. Refrig.,* 2005, 28, 859-871.

[5] Liu Y.L. and Wang R.Z., Performance prediction of a solar/gas driving double effect LiBr-H_2O absorption system. *Renewable Energy,* 2004, 29, 1677-1695.

[6] Duffie J.A. and Beckman W.A., *Solar engineering of thermal processes*, 2nd ed., Chapter 15, 1991, pp.588-619. John Wiley & Sons, New York, USA.

[7] Worsoe-Schmidt P., A solar-powered solid-absorption refrigera-tion system. *Int. J. Refrig.,* 1979, 2, 75-82.

[8] Erhard A. and Hahne E., Test and simulation of a solar-powered absorption cooling machine. *Solar Energy*, 1997, 59,155-162.

[9] Romero R.J., Rivera W., Pilatowsky I. and Best R., Comparison of the modeling of a solar absorption system for simultaneous cooling and heating operating with an aqueous ternary hydroxide and with water/lithium bromide. *Sol. Energy Mater. & Sol. Cells* , 2001, 70, 301-308.

[10] Rivera C.O. and Rivera W., Modeling of an intermittent solar absorption refrigeration system operating with ammonia/lithium nitrate mixture. *Sol. Energy Mater. &Sol. Cells,* 2003, 76, 417-427.

[11] Medrao M., Bourouis M. and Coronas A., Double-lift absorption refrigeration cycles driven by low-temperature heat sources using organic fluid mixtures as working pairs. *Appl. Energy,* 2001, 68,173-185.

[12] Fatuh M. and Murthy S.S., Comparison of R22-absorbent pairs for vapor absorption heat transformers based on P-T-X data. *Heat Recovery Systems and CHP.*,1993, 13, 33-48.

[13] He L.J., G.M. Chen X.L. Cui, Vapor-liquid equilibria for R22 +N, N-dimethylformamide system at temperatures from 283.15 to 363.15K. Fluid Phase Equilibria, 2008, 266, 84-89.

[14] Cui X.L. Chen G.M., Experimental Vapor Pressure Data and a Vapor Pressure Equation for N,N-Dimethylformamide. *J. Chem. Eng. Data,* 2006b, 51, 1860-1861.

[15] Huang B.J., Petrenko V.A., A study of ejector refrigerator system design for solar cooling application, in: A.A.M. Sayigh (Ed.), Renewable Energy. Renewables: The Energy for the 21th Century. Part Ⅱ, Peranmon, 2000, 1052-1055.

[16] Cui X.L., Theoretical and Experimental Study on Phase Equilib-rium of Novel Absorption Refrigerants. PhD Thesis of Zhejiang University, China, 2006a.

[17] Tyagi K.P. and Shankar V., Effect of Operating Variables on COP For Certain Absorbent-Refrigerant Mixtures. *ASHRAE J.*, 1976, 18, 35-38.

[18] Fathi R.,Guemimi C. and Ouaskit S., An irreversible thermody-namic model for solar absorption refrigerator. Renewable Energy, 2003, 29, 1349-1365.

978-1-935068-37-2 © 2010 SciRes.